MD-10 | 103

MILITARY TECHNICAL COLLEGE
CAIRO - EGYPT

THEORETICAL AND EXPERIMENTAL INVESTIGATION OF TUBE BULGING: PROFILE SHAPE AND LIMIT STRAINS.

S. KHORSHID*, A.R. RAGAB** & M.R. TAKLA*

ABSTRACT

This paper presents a theoretical and experimental investigation of tube-bulge-forming. The study is concerned with bulging deformations together with the limiting strains and the factors affecting instability.

Theoretical analysis considers bulging of open thin-walled tubes made of strain-hardening material. A simple approach is adopted in which the bulge profile shape is assumed to be elliptical and the ellipticity ratio is obtained by calculating the constant pressure required to retain this assumed profile shape. Results obtained according to this assumption and the assumption of circular profile shape when compared with bulging experiments of commercially pure aluminium tubes, reveal that the actual profile shape approaches an elliptical arc rather than being circular.

Limiting strains during tube bulging have also been investigated for long tubes subjected to an internal hydrostatic pressure together with an external axial force. A strain instability criterion which takes into consideration the inevitable geometrical defects in the tube-wall is developed. The results revealed that small eccentricities produce a substantial decrease in the amount of deformation sustained by the tube at instability conditions. Moreover, the sensitivity to such defects increases for tubes made of low strain-hardening materials. The developed strain instability criterion has been subjected to an experimental verification where commercially pure alumimium tubes have been bulged to fracture. Experimental results are found to be in good agreement with theory, thus justifying the validity of this instability criterion and the resulting limit strains.

INTRODUCTION

The bulge-forming of thin-walled tubes has two application, one is related to industry while the other is related to material testing. In industry, the bulge-forming technique is utilized to produce tubes with curved profile shapes from straight cylindrical ones. Tube-bulging under internal pressure combined with axial upsetting pressure allowed high expansions to be obtained in one operation |1| and |2| .

* Dept. Mech. Design & Prod. Engineering - Cairo University. Giza, Egypt.
** College of Engineering, Kuwait University, Kuwait.

As for material testing and evaluation, the bulge test of thin tubes has been utilized to obtain the stress-strain characteristics of strain-hardening materials |3| and |4|.

The problem of hydrostatic bulging of thin-walled tubes has been experimentally and theoretically studied by a number of investigators |5-10| . In their investigations, they were mainly interested in the prediction of bulge profiles, stresses, strains and thickness distributions. Some of them |6| and |7| extended their work to predict the limiting deformations and the bursting pressures. Weil |6| presented a theoretical study for the case of a closed tube having finite length and subjected to an internal pressure. His solution was based on the assumption of circular deformed meridional profile. The study was extended to investigate the maximum pressure instability at the bulge crown. Banerjee |7| , using the same assumptions was able to study the limiting deformations in bulge-forming of short tubes. His experiments on impact extruded and annealed aluminium tubes indicated large discrepancy between measured and theoretical bulge diameters for short tubes. A gerneral numerical method of analysis was suggested by Woo |8| for axi- symmetric forming of metallic shells. The analysis showed that the ratios for the principal strains remain nearly constant during the forming process and accordingly, the total strains may be directly utilized in analysis. The solution did not however satisfy the boundary conditions due to the large accumulative errors produced at the boundaries during successive computational iterations.

According to the available literature of bulging mechanics, the analysis have been limited to the assumption of a circular profile shape whose validity has been only checked during bulging of rate-dependent superplastic tube |9|. It was found that a hypothetical constraining outside non-uniform pressure was needed to maintain circular profile shape. The validity of the assumption of circular bulge profile shape for tubes made of strain-hardening materials has not been checked and no other configurations for the tube bulge profile were considered.

As for the limiting deformations, the study of plastic instability of long thin-walled tubes shows to be of a prime interest and has been considered by many investigators |10-13| . Swift |10| considered the plastic instability of closed thin-walled tube subjected to internal pressure and independent axial tensile force. He assumed instability to occur when both the internal pressure and the axial load reach a maximum simultaneously. His analyses were extended by Mellor |11| who assumed instability to occur when there is a maximum in either the total axial load or in the internal pressure. Both of them considered instability as a broadly and symmetrically distributed flow that produces uniform shell-thinning termed as diffuse necking without any reference to localised defects in the orignal tube.

The instability of a thin tube subjected to internal pressure, torsion and axial tension, all of which are independent of each other has been considered by Storakers |12| . The analysis was carried out for a strain- hardening material, and the system was defined to be fully stable if small loading perturbations cause only small changes in configuration. It was shown that stability may be lost without either of the loads attaining a maximum, but the results obtainded when the torsion stresses are excluded reduced to the same criterion previously obtained by Swift |10| . Franklin |12|, assumed instability to occur when inhomogeneity of section begins to deform faster than the bulk material. His results for non-strain-rate sens-

itive materials are not consistent with the previously obtained criterion based on maximum pressure condition. An instability criterion which corresponds to a state when an element of the sheet metal can no longer transmit plastic strain to its neighbouring element has been developed by Kaftanoglu [13]. This criterion could not be analytically expressed and a large computer program with extensive calculations was required to solve the problem.

The analysis of stability loss and the phenomenon of localized necking, for states of stressing between plane strain and equi-biaxial tension condition have been presented by Marciniak and Kuzynski [14]. Instability was assumed to take place as a result of an initial inhomogenity in the sheet metal which could simply be a thickness nonuniformity. Marciniak's theory [15] and [16] has been further discussed by several investigators, but its application to the case of thin-walled tube bulging instability was not considered by any of them.

In this work, the problem of thin-walled tube bulge forming is investigated theoretically and experimentally to get both the free-bulge profile shape and the limiting deformations. An elliptical bulge profile satisfying the conditions of equilibrium, continuity, material flow rules and boundary conditions is proposed for open short tubes subjected to internal pressure. The ellipticity ratio is chosen so that the uniformity of the pressure distribution inside the tube is satisfied. Moreover, a realistic instability criterion based on considerations of initial thickness defects which are highly probable in seamless tube production, material properties and mode of loading is suggested for long open tubes subjected to internal pressure and independent axial load. In the experimental investigation, the results, obtained by bulging aluminium tubes having different length over diameter ratios are used to examine the validity of both the proposed theoretical bulge profile shape and the developed instability criterion.

ANALYSIS

Prediction of Bulge Profile and Thickness Distribution

The equilibrium conditions for axisymmetric thin shells where radial, bending and shear stresses are small in comparison to the membrane stresses, reduce to [17] .

$$\frac{d}{d\phi}(r\sigma_\phi t) - \sigma_\phi t R \cos\phi = 0 \qquad (1\text{-a})$$

$$\sigma_\phi/R + \sigma_\phi/r_c = p/t \qquad (1\text{-b})$$

Combining both equations and integrating yields with reference to Fig.1,

$$\sigma_\phi = \frac{pr_c}{2t}\,\frac{r^2 - r_o^2}{r^2} \qquad (2\text{-a})$$

$$\sigma_\phi \quad \frac{pr_c}{2t}\left(\frac{2r^2}{r^2-r_o^2} - \frac{r_c}{R}\right)\left(\frac{r^2-r_o^2}{r^2}\right) \qquad (2\text{-b})$$

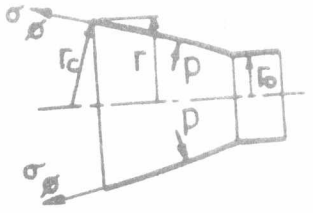

Fig.1 - Equilibrium of a bulged tube

The stress ratio α is defined as :

$$\alpha = \sigma_\phi/\sigma_\theta = \frac{R(r^2 - r_o^2)}{2Rr^2 - r_c(r^2-r_o^2)} \qquad (3)$$

The equivalent stress given by $\sigma_e^2 = 3\sigma'_{ij}\ \sigma'_{ij}/2$, thus simplifies using eq. (3) to:

$$\sigma_e = \sqrt{1-\alpha+\alpha^2}\ \sigma_\theta \qquad (4)$$

The strain components at any point of the tube wall are given by:

$$\varepsilon_\theta = \ell n\ (r/r_o) \quad \text{and} \quad \varepsilon_t = \ell n\ (t/t_o) \qquad (5)$$

Applying the constant volume condition namely: $\varepsilon_{ii} = 0$ yields for the current thickness

$$t = t_o\ \exp\{-(1+\varepsilon_\phi/\varepsilon_\theta)\varepsilon_\theta\} \qquad (6)$$

The equivalent strain defined by $\varepsilon_e^2 = 2\varepsilon_{ij}\ \varepsilon_{ij}/3$, reduces by virtue of the constant volume condition to:

$$\varepsilon_e = (4/3)\ (\varepsilon_\phi^2 + \varepsilon_\phi\varepsilon_\theta + \varepsilon_\theta^2)^{\frac{1}{2}} \qquad (7)$$

Lévy-Mises flow rule $\varepsilon_{ij} = (3\ \varepsilon_e/2\sigma_e)\ \sigma'_{ij}$ may be thus rewritten as:

$$\frac{\varepsilon_\theta}{(2-\alpha)} = \frac{\varepsilon_\phi}{(2\alpha-1)} = \frac{-\varepsilon_t}{(1+\alpha)} = \frac{\varepsilon_e}{2\sqrt{1-\alpha+\alpha^2}} \qquad (8)$$

and hence

$$\varepsilon_e = 2\varepsilon_\theta\ \sqrt{1-\alpha+\alpha^2}/(2-\alpha) \qquad (9)$$

For a strain-hardening material the behaviour is often represented by:

$$\sigma_e = \sigma_o\ \varepsilon_e^n \qquad (10)$$

Eqs. (4) and (9) are thus combined with eq. (10) to yield:

$$\sigma_\theta = \sigma_o\ \left(\frac{2}{2-\alpha}\right)^n\ (1-\alpha+\alpha^2)^{\frac{n-1}{2}}\ \varepsilon_\theta^n \qquad (11)$$

From eqs. (2-b) amd (11); employing eq. (5), the bulging pressure is expressed as :

$$p = \sigma_o t_o \left(\frac{2\ell n\ r/r_o}{2-\alpha}\right)^n\ (1-\alpha+\alpha^2)^{\frac{n-1}{2}}\ \left(\frac{r_o}{r}\right)^{\frac{1+\alpha}{2-\alpha}}\ \left(\frac{\alpha r_c + R}{r_c R}\right) \qquad (12)$$

In order to proceed further with the analysis the current profile shape for the deformed tube has to be assumed.

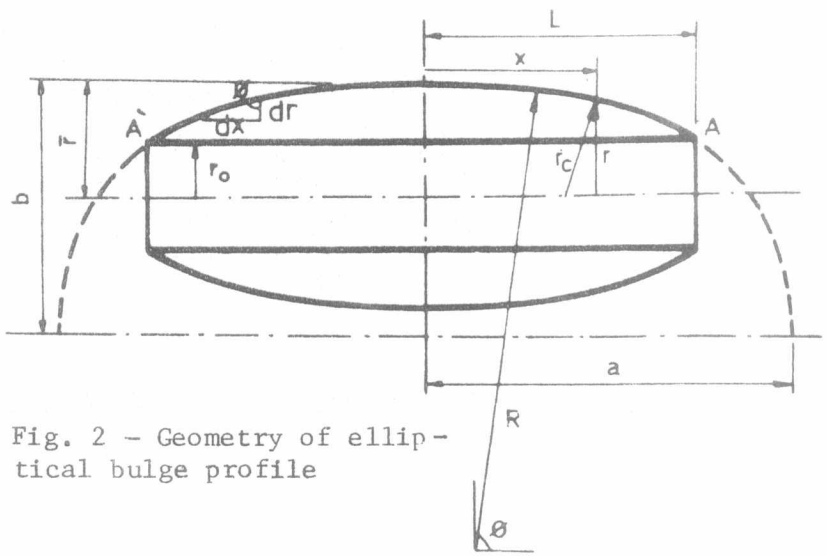

Fig. 2 – Geometry of elliptical bulge profile

a. Elliptic Profile Shape

Assuming elliptic profile as shown in Fig. 2- the geometry at any point may be described by:

$$r = \bar{r} - (b/a)\sqrt{a - (a^2 - x^2)} \quad \text{or} \tag{13}$$

$$R = \{a^4 - x^2(a^2 - b^2)\}^{3/2} / a^4 b \tag{14}$$

where $w = b/a$ is the ellipticity ratio .

The second radius of curvature is obtained from eq. (13) according to

$$r_c = r/\sin\phi = r\sqrt{1 + (dr/dx)^2} = r(abR)^{1/3} / \sqrt{a^2 - x^2} \tag{15}$$

Eqs. (13), (14) and (15) give the current tube radii of curvature at any profile point as far as the ellipticity ratio w is defined.

Substituting R and r_c in eq. (12) and rearranging results in:

$$p = \frac{\sigma_o t_o}{r_o} \frac{2r^2\alpha}{r^2 - r_o^2} (1 - \alpha + \alpha^2)^{\frac{n-1}{2}} \left(\frac{2 \ell n\, r/r_o}{2-\alpha}\right)^n \left(\frac{r}{r_o}\right)^{\frac{3}{\alpha-2}} \frac{\sqrt{a^2 - x^2}}{(abR)^{1/3}} \tag{16}$$

b. Circular Profile Shape

If the assumption of circular bulge-profile shape proposed in the literature was adopted, the solution is obtained by substituting $(w = b/a = 1.0)$ in the group of equations (13) to (15). The corresponding pressure distribution is thus given by:

$$p = \frac{\sigma_o t_o}{r_o} \frac{2r^2\alpha}{r^2 - r_o^2} (1 - \alpha + \alpha^2)^{\frac{n-1}{2}} \left(\frac{2 \ell n\, r/r_o}{2-\alpha}\right)^n (R^2 - x^2) \left(\frac{r}{r_o}\right)^{\frac{3}{\alpha-2}} \tag{17}$$

Eq. (16) gives the theoretical pressure at any position along the tube axis for a certain value of the crown radius $\bar{r}$ and ellipticity ratio w. For bulging with hydrostatic pressure, there is obviously no variation of pressure along tube length. Adopting an inverse method of solution [18], the validity of the assumptions concerning the bulge profile shape could be checked. An assumed profile shape which is close to reality must produce constant pressure distribution along the tube length at any deformation stage. For instance this check is achieved through solving eq. 16 and the bulging pressure P_o at the crown (x= 0) is obtained from same eq. . Another value for the pressure (designated by p_1) is obtained near the tube end i.e. at x/L = 0.95. If p_1 is different from p_o then, the assumed ellpticity is modified and the procedure is repeated until the relation $p_o \simeq p_1$ is realized. The same method of solution could be applied to the circular profile using eq. (17).

Prediction of Limit Strains

The mode of instability considered here assumes that at a certain moment while bulging, some selected sections continue to deform while others begin to unload [14] . That phenomenon may occur due to the presence of an infinitesimal thickness variation in the tube due to either manufacturing imperfections or microstructural inhomogeniety. The section having minimum thickness will be the most stressed one at which stability loss is predicted to occur. But, at early stages of loading, all sections are fairly subjected to equal stress values with infinitesimal differences.

In the appendix the strain instability criterion as developed in reference [19] is applied to a long thin-walled tube of localized wall defect and the condition of instability is found to be:

$$d\,\sigma_{\theta I} / \sigma_{\theta I} + dt_I / t_I = 0 \qquad (18)$$

For a strain-hardening material of behaviour represented by $\sigma_e = \sigma_o \varepsilon_e^n$ the limit strains are given by:

$$\varepsilon_\theta = (2-\alpha / 1+\alpha)n$$

$$\varepsilon_\theta = (2\alpha - 1 / 1+\alpha)n \qquad (19)$$

$$\varepsilon_t = -n$$

In the solution obtained above, it is assumed that the tube thickness is initially homogeneous, and that instability takes place due to the presence of an infinitesimally small geometrical inhomogeniety in the tube wall.

In general, most tubes are of a non-uniform thickness (t) which could be described as a function of the element position (θ) around the periphery namely : $t = t(\theta)$. For eccentrically drawn tubes - Fig. 3 the initial thickness distribution may be represented by the equation:

$$t_o = T_o - \Delta \cos \theta_o \qquad (20)$$

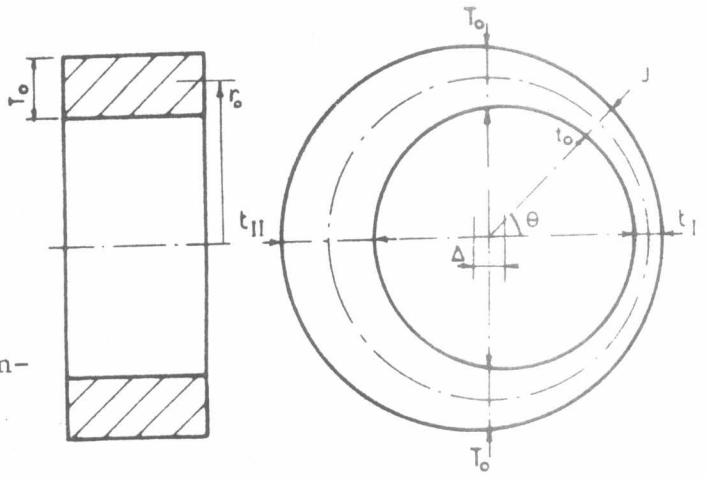

Fig. 3 - Geometry of thin-walled tube with initial eccentricity.

where T_o and Δ are the initial average thickness and initial eccentricity respectively while θ_o is the angular position referred to the section of minimum thickness.

The tangential strain and strain increment at any point is respectively given by:

$$d\varepsilon_\theta = d(r\, d\theta) / (r\, d\theta) \tag{21}$$

and

$$\varepsilon_\theta = \ell n \{(r\, d\theta) / (r\, d\theta)_o\}$$

where r is the current mean radius of the tube and r_o is the original mean radius. It must be taken into account that $d\theta$ differs from $d\theta_o$ since obviously the material point does not move radially during deformation of tubes having non-uniform thickness. Both ε_θ and $d\varepsilon_\theta$ are functions of θ and are not uniform along the circumferential profile. Now, considering an average circumferential strain, defined by:

$$\bar{\varepsilon}_\theta = \ell n\, (r / r_o) \tag{22}$$

Utilizing eq. (21) and integrating along the circumferential profile, yields:

$$\bar{\varepsilon}_\theta = \ell n \frac{r}{r_o} = \ell n \{ \frac{1}{2\pi} \int_o^{2\pi} \exp(\varepsilon_\theta)\, d\theta_o \tag{23}$$

The thickness strain (ε_t) and its increment are functions of θ and given by:

$$\varepsilon_t(\theta) = \ell n\{ t(\theta) / t_o(\theta)\} \tag{24}$$

According to the strain instability criterion presented in the Appendix, instability takes place at the weakest section while other sections start to unload. Hence the same instability condition as given by eq. (18) could be applied. For small orders of thickness varition, the stress and strain ratios may be assumed to remain constant for all sections so that the integrated form of the Levy-Mises flow rule applies. According to the assumption of uniform distribution of stress ratio together with proportional loading conditions, eq. (4) applies. Utilizing eq. (24), the instability condition (18) reduces to:

$$d\varepsilon_{tI} = - d\sigma_{eI} / \sigma_{eI} \qquad (25)$$

Substituting the plastic stress-strain relations, eq. (8) in eq. (25), gives:

$$d\varepsilon_{tI} = - \frac{d\sigma_{eI}}{\sigma_{eI}} = - \frac{-(1+\alpha)}{2\sqrt{1-\alpha+\alpha^2}} d\varepsilon_{eI} \qquad (26)$$

Using eq. (9) together with eq. (10) and substituting into eq. (26), the instability strains at the section originally having minimum thickness will be the same as previously obtained for a tube with localized defect and given by eqs. (19) . Referring to Fig. 3, and considering the general section (J), having position angle (θ), and assuming the same curvature for both sections I and J, then, at any stage of deformation, it may be written:

$$\sigma_{\theta I} \cdot t_I = \sigma_{\theta J} \cdot t_J \qquad (27)$$

Combinging eqs. (24) and (27) for sections I and J and rearranging yields:

$$\sigma_{\theta I} / \sigma_{\theta J} = (t_J / t_I)_o \exp (\varepsilon_{tJ} - \varepsilon_{tI}) \qquad (28)$$

According to the assumption of uniform stress ratio, it may be seen that:

$$\sigma_{\theta I} / \sigma_{\theta J} = (\varepsilon_{tI} / \varepsilon_{tJ})^n \qquad (29)$$

Substituting eq. (29) into eq. (28) and then rearranging yields:

$$(t_J / t_I)_o = (\varepsilon_{tI} / \varepsilon_{tJ})^n \exp (\varepsilon_{tI} - \varepsilon_{tJ}) \qquad (30)$$

Substituting from eq. (19) into eq. (30) gives for any section (J):

$$(t_J / t_I)_o = - (n/\varepsilon_t)^n \exp (-n - \varepsilon_{tJ}) \qquad (31)$$

Referring to the thickness distribution given by eq. (20) yields:

$$t_{IO} = T_o - \Delta \qquad (32)$$

Also, rewriting eq. (20) in terms of t_{IO} produces;

$$(t / t_I)_o = 1 + (\Delta / t_{IO}) (1 - \cos \theta_o) \qquad (33)$$

Substituting eq.(33) into eq.(31) and rearranging , results in:

$$\cos \theta_o = 1 - \left(\frac{T_o}{\Delta} - 1\right)\left\{\left(\frac{-n}{\varepsilon_t}\right)^n \exp\left(-n - \varepsilon_t\right) - 1\right\} \quad (34)$$

Substituting eq. (8) into eq. (29) gives:

$$\cos \theta_o = 1 - \left(\frac{T_o}{\Delta} - 1\right)\left\{\left(\frac{2-\alpha}{1+\alpha}\,\frac{n}{\varepsilon_\theta}\right)^n \exp\left(\frac{1+\alpha}{2-\alpha}\,\varepsilon_\theta - n\right) - 1\right\} \quad (35)$$

This equation defines the local strains ε_θ at any section knowing initial distribution of thickness i.e. T_o, Δ, θ, the stress ratio α and the material hardening exponent n. Using this distribution of $\varepsilon_\theta(\theta)$ in eq. (23), the mean current radius at instability is obtained by integration. A good approximation is to take $\exp(\varepsilon_\theta)$ in polynomial form of θ as:

$$\exp(\varepsilon_\theta) = \exp\left(\frac{2-\alpha}{1+\alpha} n\right) + \Sigma a_k \theta^k \quad (36)$$

where the first constant gives ε_θ at section I independently of (Δ/T_o) as obtained from the analysis in the Appendix. A reasonably selected number of constants a_k could be determined for each specific case by curve fitting. The tube radius at instability is then obtained by direct integration of eq. (36) i.e.:

$$(r/r_o)\ \text{instability} = \exp\left(\frac{2-\alpha}{1+\alpha} n\right) + \Sigma a_k \pi^k/(k+1) \quad (37)$$

RESULTS AND COMPARISON WITH EXPERIMENTS

Experiments

Experimental work was conducted to inspect the validity of the derived theoretical relations given above. The experimental investigation, deals with two basic parts. In the first part, free bulging of open tubes was performed by applying an internal pressure together with a negligibly small axial load which was directly applied on the tube walls. Experiments for bulging of tubes having L/r_o values of 0.5, 1.0 and 3.0 were conducted. The bulged tubes were thereafter carefully split so that the profile shape and thickness distribution were measured. The results are compared with elliptic and circular profile shapes and their corresponding thickness distribution.

The second part deals with instability where initial thickness variation plays the most important role. Specimens were arranged in groups having different values of (Δ/T_o) ranging from 0.015 to 0.17. Measurements were limited to tubes having L/r_o value of 3.0. Hydrostatic bulging was performed with a constant axial load and bulge-diameters at instability were

measured. Results are compared with the predictions of eq. (37). A group of experiments was performed under the same loading conditions to measure the effect of the tube thickness variations on the instability diameter. while another group of experiments was conducted on tubes having almost similar thickness variations to measure the effect of the axial load on limiting deformations.

Test specimens were extruded seamless tubes produced by further sinking to 25 mm external diameter and 1.0 mm nominal thickness. The tube material which is commercially pure aluminium (99.7% Al) was found to have a flow curve equation given by:

$$\sigma_e = 145\ \varepsilon_e^{0.25} \quad \text{(MPa)} \qquad (38)$$

A test rig for tube-bulging process was constructed so that an axial load can be applied independent of the hydrostatic pressure. Vulcanized rubber was utilized, instead of oil as a bulging medium so that the problems of sealing could be avoided.

Results:

Bulge Profile and Thickness Distribution

The experimentally uniform pressures used to bulge tubes having L/r_o values of 0.5, 1.0 and 3.0 are presented in Fig. 4 with the associated theoretical pressure distributions as predicted by both the proposed solution - eq. (18)- and that according to the assumption of a circular profile shape, eq. (19). Inspection of the given curves reveals that the proposed solution is in good agreement with experimental results for the range of x/L from zero upto 0.95 with maximum deviations, within 4-12% from the experimental pressures. Meanwhile the solution according to the assumption of circular profile gives within the same range of x/L, maximum deviations ranging from 8-26%. These results favour the proposed solution over the often-made assumption of circular profile.

In Fig. 5, the experimental bulge profiles are drawn together with both the proposed elliptical profile solution and the circular profile for the same values of $L/r_o = 0.5$, 1.0 and 3.0. These curves indicate that the proposed solution satisfactorily agrees with the experimental profile with maximum deviations of 4.4% , 2.1% and -13.25% for crown expansion. Meanwhile the circular profile gives within the same range of x/L, maximum deviations of - 16.2%, - 18.3% and - 36% respectively.

The experimental thickness distribution of the deformed tubes is plotted in Fig. 6 along the tube axis together with the proposed theoretical distribution and that corresponding to the assumption of a circular profile. For L/r_o values of 0.5, 1.0 and 3.0 it may be seen that the proposed solution gives thickness distributions in good agreement with experiments for the range of x/L from zero upto 0.9. Again, these results favour the proposed elliptical profile over the assumption of circular profile for which the maximum error is about 18% for the range of x/L from zero upto 0.9.

Limiting Strains

a) Effect of Initial Thickness Defects:

In order to experimentally investigate the effect of tube geometrical defects, the test tubes were classified according to the original thickness variation Δ from the mean thickness T_o-eq. (20). Groups of specimens having values of (Δ/T_o) in the range of 0.015 to 0.17, are bulged to failure under the same conditions of loading. The bulged tubes which are of the same material, have also the same dimensions of 25 mm external diameter, 1.0 mm mean thickness and 72 mm free bulge length, thus producing L/r_o values of 3.0 for all the specimens.

The effect of thickness varition of tube-bulging instability is clarified in Fig. 7. The experimental results are plotted with both the developed theoretical solutions and the expected values from literature, for the range of Δ/T_o from 0.015 upto 0.17. Inspection of these curves shows that the proposed solution gives good agreement for this range. The solution for a tube having an initially small localized thickness defect, which neglects ecoentricity, eq. (19) overestimates the instability strains. Swift instability criterion [10] as well as Mellor criterion (maximum pressure) underestimate the expected instability diameter. Inspite of this fact, these theories were, accidentally, in good agreement with the experimental results for the range of Δ/T_o from 0.12 upto 0.17 only, while for a tube having Δ/T_o = 0.015 deviations from experiments are about 60% for the two criteria.

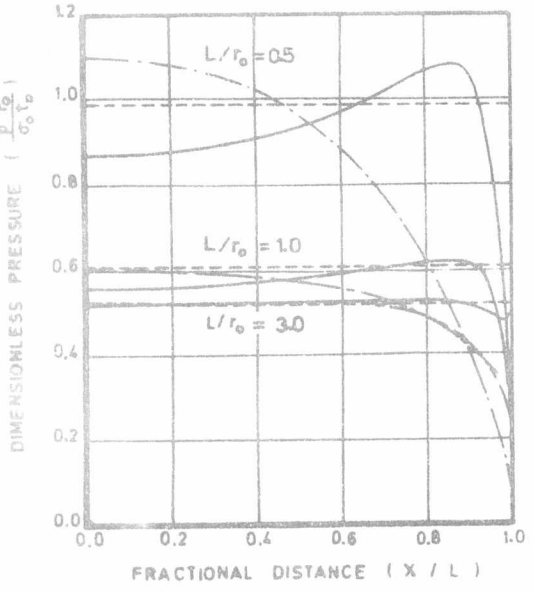

Fig. 4 - Pressure distribution along bulged tube.——— theoretical elliptical profile, ——·——·—— theoretical circular, — — — — experimental

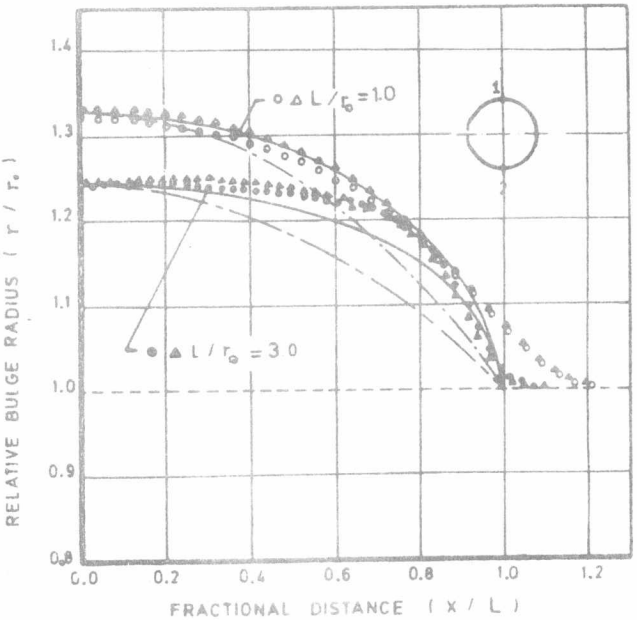

Fig. 5 - Bulge profile shape.——— theoretical elliptical profile, ——·——·—— theoretical circular profile.

b) Effect of Stress Ratio:

Fig. 8, represents the effect of the state of stress on tube instability. The experimental results are compared with both the proposed criterion and the previously suggested ones. It is seen that the theoretical

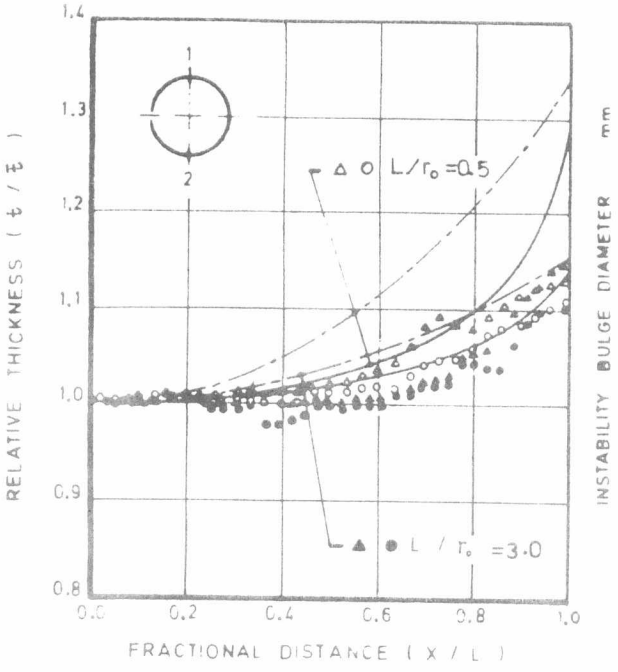

Fig. 6 - Thickness distribution along bulged tube. ——— theoretical elliptical profile, - - - - - - theoretical circular profile.

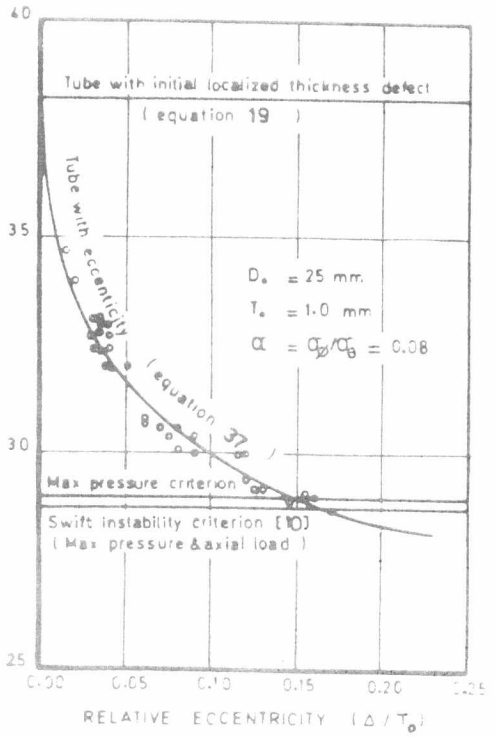

Fig. 7 - Effect of initial eccentricity on limit deformation.

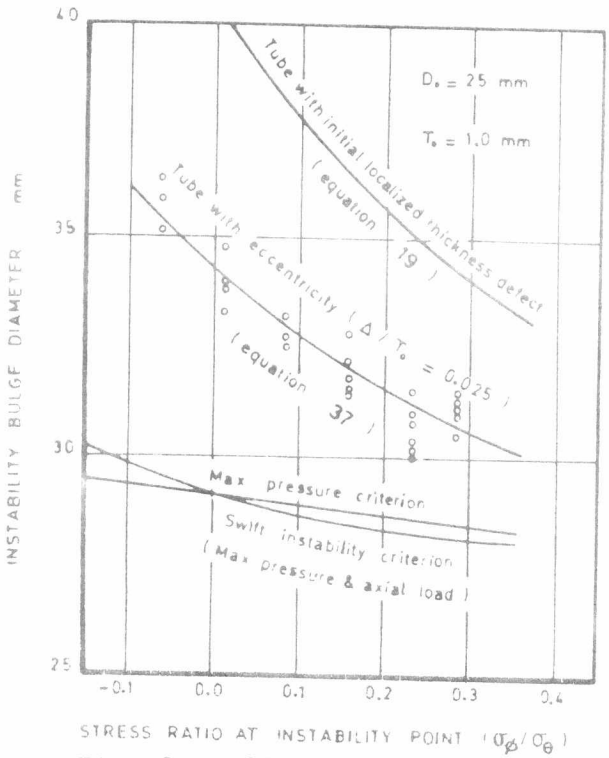

Fig. 8 - Effect of state of stress on limit deformations.

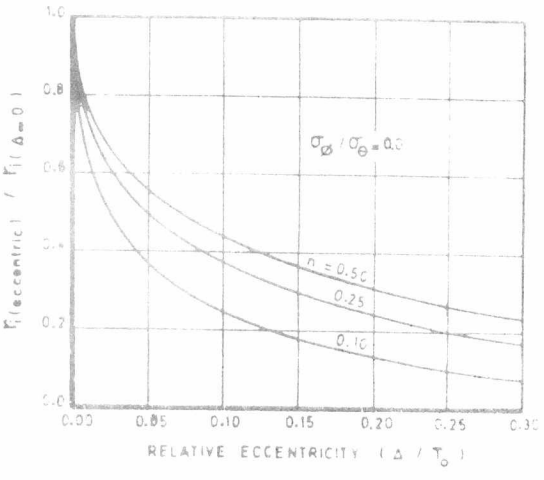

Fig. 9 - Effect of tube eccentricity on instability strain for various hardening coefficients.

solution gives good results for the range of stress ratio $\alpha = \sigma_\phi/\sigma_\theta$ from -0.1 upto 0.3. Again both the maximum pressure criterion and that of simultaneous maximum pressure and axial load, underestimate the bulge diameter with a deviation about 50% less than the obtained experimental values. They have however the same decaying trend with the stress ratio, as the experimental curves. On the other hand, the developed solution for a tube having initially a small localized thickness defect (neglecting thickness variations), overestimates the instability strains as shown in Fig. 8. It gives the same trend with a deviation of about 65% over the experimentally obtained values. Note that the experimentally obtained stress ratio α comes from actual load cell measurements at the instability point.

c) Effect of Strain - Hardening Exponent

The effect of tube sinking eccentricity on maximum diametral expansion at instability is found to be very harmful even for very small values n as shown in Fig. 9. The drop in ductility becomes less pronounced for further increase of Δ/T_o. The sensitivity of bulging instability to tube eccentricities is also clarified for different tube materials. Comparison reveals that materials having lower strain-hardening exponents are more sensitive to sinking eccentricities.

CONCLUSION

In the theoretical analysis, the bulge profile shape of thin walled tubes, is assumed to be elliptical. The required pressures and the resulting thickness distributions are compared with those obtained according to the often-made assumption of circular profile shape. The experimentally obtained bulge profile shapes, bulging pressures and thickness distributions for commercially pure aluminium tubes are compared with the theoretical results given by both assumptions. The comparison favours the assumption of elliptical profile shape over the circular one for all values of tube length diameter ratios.

A strain instability criterion which takes into consideration the inevitable geometrical local defects in the tube wall has been developed and the effect of radially continuous thickness defects on tube-bulging instability has been thus investigated. The results indicate that small eccentricities produce a substantial decrease of the amount of deformation sustained by the tube at instability conditions. The developed strain instability criterion has been subjected to an experimental verification where commercially pure aluminium tubes produced by extrusion and further sinking have been bulged to fracture. Experimental results are found to be in a good agreement with the theoretical assumptions given before. This justifies the validity of this instability criterion together with the related analysis considering the effect of initial tube geometrical defects on the limiting deformations.

REFERENCES

1. Wallick, C.R., "Tube bulging with axial pressure " Metal working production, pp. 52 , July, (1965)
2. Limb, M, Mellor, P.B. and Garber, S., "End forming of tubes with polyurethene", Int. J. Mach. Tool Des. Res., (1970)
3. Woo, D.M. and Hawrkes, P.J., "Determination of stress-strain characteristics of tubular materials", J. Inst. Metals, 96, pp. 357, (1968)
4. Jones, B.H. "Assessing instability of thin-walled tubes under biaxial stresses in the plastic range", Exp. mech., pp. 10-18, January, (1968)
5. Woo, D.M. "Tube-bulging under internal pressure and axial force", J. Eng. Mat. and Tech. Trans. ASME, 1, pp. 1-5 (1973)
6. Weil, N.A. "Tensile instability of thin-walled cylinders of finite length", Int. J. Mech. Sci, 5, pp. 487-506, (1963)
7. Banerjee, J.K., "Limiting deformations in bulge-forming of thin cylinders of fixed length", Int. J. Mech. Sci, 17, pp.659-662, (1975)
8. Woo, D.M., "The analysis of axi-symmetric forming of sheet metal and the hydrostatic bulging process", Int. J. Mech. Sci, 6, pp. 303, (1964).
9. Ragab, A.R. "Analysis of rate- dependent bulging of superplastic tubes" Current advances in Mechanical Design & Production edited by G. Shawki and S. Metwalli, Pergamon Press, pp. 247, (1981)
10. Swift, H.W., "Plastic instability under plane stress,, J. Mech. Phys. Solids, 1. pp.1. (1952)
11. Mellor, P.B., "Plastic instability in tension", The Engineer, March (1960)
12. Storakers, B., "Plastic and Visco-plastic instability of thin tube under internal pressure, torsion and axial tension", Int. J. Mech. Sci., 10, pp.519 - 529, (1968).
13. Kaftanoglu, B., "Plastic instability of thin shells deformed by rigid punches and by hydraulic pressure ", J. of Eng. Mat. and Tech., Trans ASME , pp. 36, (1973).
14. Marciniak, Z., Kuczynski, K., "Limit strains in the process of stretch forming sheet metal", Int. J. Mech. Sci, 9, pp. 609-620 (1967).
15. Sowerby, R., and Duncan, J.L., "Failure in sheet metal in biaxial tension", Int. J. Mech. Sci, pp. 217 , (1971).
16. Marciniak, Z., Kuczynski, K., and Pokora, T., "Influence of the plastic properties of a material on the forming limit diagram for sheet metal in tension", Int. J. Mech. Sci, 15, pp. 789-805 (1973)
17. Flügge, W., "Stress in shells", Springer-Verlag, New York, (1973).
18. Timoshenko, S., Theory of plates and shells, Mc-Graw Hill, New York, (1940).
19. Ragab, A.R., Khorsheid, S.A. and M. Takla, "On the plastic instability of thin-walled tubes", Proc. of 2nd MDP Conference, Cairo University, Egypt, pp. 541, Dec. (1982).

NOMENCLATURE

a	Major radius of the ellipse
b	Minor radius of the ellipse
L	Current tube half - length
n	Strain-hardening coefficient
p	Internal pressure
R	Meridional radius of curvature at any position (x)
r_c	Second radius of curvature at a general section.
r	Deformed tube radius at any position (x)
$\bar{r}$	Deformed tube radius at the crown (x=0)
r_o	Undeformed tube radius

T_o Initial average tube thickness
t_o Initial tube thickness at angular position (θ)
t^o Tube thickness at angular position (θ).
w Ellipticity ratio (b/a)
x Current axial position of a point referred to the crown
α The stress ratio ($\sigma_\phi/\sigma_\theta$)
Δ Original tube eccentricity
θ Peripheral angular position
ϕ Meridional angular position
σ True stress
σ_e Effective stress
σ_o Material strength parameter
ε^o Natural strain
ε_e Equivalent strain
$\bar{\varepsilon}_\theta$ Average circumferential strain

APPENDIX

Considering a thin-walled tube of a thickness defect where region (I) represents an infinitesimal defect, while region (II) is of uniform thickness the following equilibrium condition could be written:

$$\sigma_{\theta I} = pr/t_I \qquad (39\text{-a})$$

$$\sigma_{\theta II} = pr/t_{II} \qquad (39\text{-b})$$

Rearranging, taking logarithms and differentiating gives:

$$d\sigma_{\theta I}/\sigma_{\theta I} + dt_I/t_I - dr_I/r_I = d\sigma_{\theta II}/\sigma_{\theta II} + dt_{II}/t_{II} - dr_{II}/r_{II} \qquad (40)$$

According to the definition of strain instability, the limit strain is reached when section II begins to unload while section I continues to deform, i.e. the stress carried by section II reaches a maximum and its further plastic deformation stops, then;

$$d\sigma_{\theta II} = dt_{II} = 0 \qquad (41\text{-a})$$

At the instant when strain instability is just reached, any additional deformation in the weak section (I), results in an increase of the radius of curvature of all sections. However, according to the membrane theory which holds for thin-walled sections, bending stresses that may cause changes in curvature are neglected. In addition, since the wall thickness variations are initially assumed to be infinitesimally small, thus, curvatures of all sections and their rates of change can be assumed to remain instantaneously the same. Hence, at the condition when strain instability is just reached it may be written:

$$dr_I = dr_{II} \qquad (41\text{-b})$$

It must be noted here that the strain instability condition is independent

of that of maximum pressure and it may be reached after a period of uniform deformation under falling pressure.

Substituting eqs. (41-a) and (41-b) into eq. (40) results in:

$$d\sigma_{\theta I} / \sigma_{\theta I} + dt_I / t_I = 0 \qquad (42)$$

Eq. (42) indicates that the strain instability criterion gives the same expression which could be obtained according to maximum wall strength in hoop direction.

Rearranging eq. (42) and employing the material behaviour law, eq. (10) yields:

$$\varepsilon_{eI} = - (d \varepsilon_{eI} / d\varepsilon_{tI})n \qquad (43)$$

At the moment, when instability just takes place, thickness variations are still infinitesimal and equation (43) can be written for any section by dropping the subscript I. Substituting the plastic stress – strain relations given by eq. (8) into eq. (43) produces:

$$\varepsilon_e / n = 2\sqrt{1-\alpha+\alpha^2} / (1+\alpha) \qquad (44)$$

Eq. (44) gives a measure of the strain instability condition as function of the loading stress ratio α and the material strain-hardening exponent n.

Combining eq. (44) with eq. (8), the limit strains corresponding to the strain instability criterion are given by :

$$\varepsilon_\theta = (2 - \alpha / 1 + \alpha) \, n$$

$$\varepsilon_\phi = (2\alpha - 1 / 1 + \alpha) \, n \qquad (45)$$

$$\varepsilon_t = - n$$